nessa publishers

Journal of Cancer Science and Therapy
Volume 1| Issue 10

Research Article **Open Access**

Monte Carlo Simulation of Infinia Gamma Camera: A Verification and Validation Process

[1]M. A. Alnafea, [2]K. Wells

[1, 2] Department of Radiological Sciences, King Saud University

[*]**Corresponding author**: M. A. Alnafea, Department of Radiological Sciences, College of Applied Medical Sciences, Riyadh, King Saud University; Email: alnafea@ksu.edu.sa

Citation: M. A. Alnafea (2018) Monte Carlo Simulation of Infinia Gamma Camera: A Verification and Validation Process: Nessa J Cancer Sci and Therapy

Received: 29th January 2018 **Accepted:** 1st February 2018 **Published:** 26th February 2018

Abstract

Radio nuclide imaging technique with Anger camera becoming widely used in the last two decades for cancer detection. Such camera often employs low energy high-resolution (LEHR) parallel-hole collimator. This paper introduces and investigates the realistic simulation and validation process for the recently installed Infina gamma camera. Monte Carlo Simulation (MCS) is using a well-known MCNPX package undertaken in this study to be later used for investigating the possible applications of collimator-less radionuclide imaging for breast tumor imaging. The modeling steps and the validation process of the simulated camera against the full-size clinical Infina gamma camera described. Such verification steps of the imaging are important and provide confidence to the simulation work. It describes the methodology used for modeling and testing the Infina gamma camera with parallel-hole collimators image formation. The obtain results using MSC and real experiment using the Infina gamma camera demonstrate accurate construction, testing and verification of the simulated geometry.

Keywords: *Monte Carlo Simulation; Gamma Camera; Parallel-hole; Validation.*

1. Introduction

In the Middle East, breast cancer is a life threatening disease and the most common malignancy among women [1-4]. Thus, considered as the second most frequent cause of cancer death [5, 6] as it constitutes ~ 14 % of female cancer deaths [7]. Unfortunately, it is incidence rates are still increasing in most countries [8]. Scintimammography (SM) with a general-purpose γ-camera recently introduced to evaluate patients with dense breast [9] prior and in a least case after breast biopsy [10]. The technique considered valuable for many clinical applications such as evaluating the axillary lymph nodes, investigating patients with micro calcifications [11]. As well as used for assessing multifocal and multi-centric breast cancer diseases [12]. It is also useful for imaging patients following surgery, chemotherapy, hormonal replacement therapy and radiotherapy as well as for patients with breast implants [9]. In summary, SM using conventional γ-camera considered as a useful complementary imaging modality to aid the diagnosis and the detection of breast cancer.

This study is based on a computational technique that attempts to model a real physical system of Infina γ-camera recently installed in radiological sciences department. This statistical calculation method based on the technique of random variable sampling that utilizes sequences of random numbers [13]. In the case of γ-ray transport problems, individual photons are tracked from point of origin to removal from the system (either by escape or by absorption), while interacting in a random way, as determined by the cross sections. Anger was the first to use this technique for simulating the physical response of his gamma camera.

Since then, the technique has gained wide spread for many nuclear medicine applications. This may include the optimization of new cameras (detector or collimator) and the evaluation of the correction and the reconstruction techniques [14, 15].

MCNP [13, 16] that stands for Monte Carlo N-Particle was chosen for this work. It is a general-purpose codes and thus, supports 34 particles (or coupled particles) types. It has many cross section libraries for di erent physics models. MCNPX (stands for MCNP extended) is the one that was chosen as it models the physics of photon transport of the imaging system in a more accurate way. It is also user friendly in term of geometrical and materials control. MCNPX (version 2.4.0) code used in this work because it explicitly models the transport and the details physical interaction of photons within the geometries simulated. The interactions of every primary and all subsequent photons and particles are tracked until they are either stopped, absorbed or leave the detection system. In other words, histories terminated when the photon escapes from the detector or when its energy dropped to the energy cut-o (1 keV).

2. Materials and Methods

2.1 Monte Carlo Basic Concepts

The package reads the input file of the specified geometry and desired calculations. It then simulates individual particle histories and records the requested information. It allows the representation of all aspects of physical data with no approximations or averaging. This means that the individual probabilistic events subject to statistical processes during interactions with various media simulated sequentially. The MCNPX code uses a built in pseudo-random number generator. The pseudo-random number generator supplies a unique sequence of numbers having an initial value called seeds. If the

same seed is used it will generate the same sequence of random number. The pseudo-random number generator has also a random number stride (period or jump). The number of random numbers between any two consecutive particle histories. The code has a default pseudo-random number stride but it can be changed on the "RAND" card so that the stride is not exceeded. As with most codes MCNPX code deal with binary numbers. A pseudo-random sequence of integers in is generated by:

$$I_{n+1} = mod\ (R_m I_n.n^{48}) \quad (1)$$

Where Rm is the random number multiplier and 48-bit integers and 48-bit floating point mantissas are assumed. The default value of Rm is 519. The pseudo-random number is given by:

$$R_n = (2^{-48}) \quad (2)$$

The starting pseudo-random number of each history is:

$$I_{n+1} = mod\ (M^s.\ I^n) \quad (3)$$

Where s is the pseudo-random number stride. The default value of s is 4525258. This number ensures that the bit pattern will change when the stride multiplied by almost anything. The period P of the MCNP algorithm is:

$$P = 2^{46} \approx 7.04 \times 10^{13} \quad (4)$$

2.1.1 Modelling the Infinia Imaging Detector

Most γ-ray imaging detectors normally operate in pulse mode [17]. It means that each detected photon represented as a pulse and the final image produced from a narrow window of particular amplitudes corresponding to a particular range of deposited energy. Thus, to simulate and accurately model the imaging detector, using the MCNPX code, one need to know the energy deposition, process by the detector as well as the spatial information that gives the exact location of photons. This achieved by combining the use of tally F8 as well as the use of a feature of the MCNPX code referred to as Particle Track Output Card (PTRAC). The former gives the energy deposition of number of pulses recorded by the detector whereas the latter gives detail interactions including the photon locations as well as their energies deposition. Both utilities provide accurate and detailed physics simulation for the imaging detector.

The following text provides a description of the steps undertaken to model the γ-ray imaging detector in a realistic way using the MCNPX code. This should also include the effects of limiting energy and spatial resolution on the projected images. These effects have been accounted for using a post simulation utility written using Mat lab. The model then validated with

experimental results so that it used as a platform with any image formation systems. Before describing the post-simulation program, a description of the PTRAC card is given. Such card in the simulation geometry of the MCNPX code produces a large output data file on particles trajectories. This single output list file, referred to as a PTRAC file has specific format. The PTRAC file sorted out first for further processing and image construction.

2.1.2 Post Simulation Program

To read the simulation data file a simple post-processing program was written [18] to extract all histories from the PTRAC ASCII file corresponding to photons which interacted in the gamma camera's NaI crystal. The code then increments the image from these data files. To achieve better efficiency the code has been slightly modified to suite different source geometries and simulation set-ups. The main structure and the theoretical principle of the original code remains the same. The code accumulates the spatial information of photons and their energies that have been finally deposited in the detector lattice. The effective position of a photon within the detector is calculated as the weighted average of the energy lost within the scintillation crystal. This is achieved by following each individual event over the position of the respective interaction using the center-of-mass principle for the calculation.

The total energy deposited within the detector is obtained by summing all the energies lost by the photon. The imperfections arising due to statistical uncertainty in position read out and in the recorded energy deposition process were also simulated using the same Mat lab code. This was achieved by sampling a Gaussian distribution. Both the energy deposited by the photon and the X and Y position information are convoluted with a random noise from a zero mean values normal distribution. This process will simply blur both the spatial information and the energy deposition. Then the code uses a specified energy window to determine whether a particular event is accepted or ignored. Thus, all the major physics aspects of the imaging system are considered. The final part of the code is to divide the detector up into a matrix of pixels to produce a 2D projected image. The code also produces simulated energy histogram.

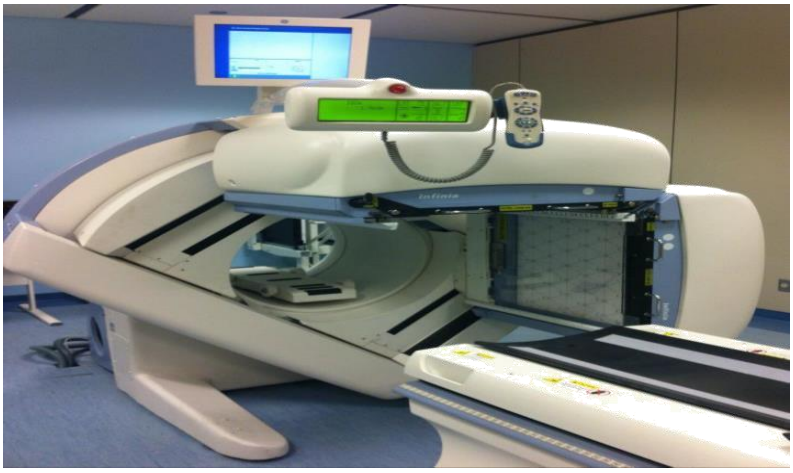

Figure 1: The Infinia Dual gamma camera

2.2 The Infinia Gamma Camera

Fig. 1 shows the Infinia dual headed gamma camera is located in the department of radiological king Saud University. Only one of the imaging detectors of the aforementioned gamma camera used in the simulated data. The camera specifications obtained experimentally or given by the manufacturers were summarized in table 1. The imaging detector of head one is a single block rectangular object whose size is 54×40 cm^2. The scintillator (crystal) is of thickness 0.95 cm and provides an experimentally (by the manufacturer) verified spatial resolution of ≈0.38 cm FWHM. The later value is the system PSF measured at the center of the crystal with an idealized point source. This means that an idealized point source is seen not as a point but as a blur or spot.

Table 1: The main parameters of the Infinia from GE Dual head system gamma camera and the Detector performance (manufacturer's specification). All the physical parameters are obtained using ^{99m}Tc point source and with its photon energy 140 keV with the LEHR collimator in place.

Main Parameters	Values obtained	Main Parameters	Manufacturer's Specification
Sensitivity (cpm/kBq)	4.3	Energy range	40 - 511 keV
Field of View (mm)	540 × 400	Field of View (mm)	540 × 400
Photomultipliers	59 tubes×76 mm diameter	intrinsic resolution	3.7 mm FWHM (Central FoV)
Scintillator	NaI (Tl) crystal	Uniformity	2.1 % (Central FoV)
Crystal thickness	9.5 mm thickness	Linearity	0.1 mm (Di)
Collimator mass (kg)	60	Energy resolution	9.8 % (Useful FoV)

2.3. Geometry

The camera was modeled following an approach suggested by Devries and Moore [19]. The first and the most important component of the camera is the collimator (see Fig. 2(a)) and were geometrically modeled as a parallel-hole having square holes (see Fig. 2 (b)) [19]. The simulated collimator was of LEHR type as such collimator is mainly used for imaging 140 keV photons. The main parameters or specifications of such collimator are given in table 2. The imaging detector consists of a 0.95 cm NaI scintillation detector with density 3.67 g/cm^3. The simulated detector is of size 40 cm ×40 cm and defined by 128^2 pixels, each 0.3125×0.3125 cm^2. The backscatter from the Photo-Multiplier Tube (PMT) array is approximated by simulating a 6.8 cm thick slab of Pyrex following the method recommended by [19]. This homogenous block of Pyrex has 66% of the density of normal Pyrex to accurately simulate the PMT array glass material. The Pyrex was positioned directly behind the camera imaging detector. Thus, all the camera components were modeled, with MCNPX code, using sets of simple geometric primitives with various materials assigned to these shapes. Finally, all the camera geometries including the source should be within a sphere used in all simulations to limit the area in which transport take place as shown in Fig. 3. In all simulations carried out in this work the sources are emitted isotropically in all directions of the geometry. The simulated photons generated in the object under study are mainly subject to Compton scattering and photoelectric effect.

The resulting photon histories, track individually, the positions of interactions and energy losses are then recorded in the PTRAC output file. The use of pulse height tallies (F8) in the input file provide the energy distribution of pulses created in the NaI crystal. The primary photons and all subsequent photons and electron particles are considered in the simulation. All these are tracked until they are either stopped entirely or leave the detector boundary. For accurate and more realistic simulation of the Infinia gamma camera, each photon must be then subject to the effects of limited photoelectron statistics reflected in the finite energy and spatial resolution. To account for these effects, specific values were utilized derived from a-priori experiments on an actual Infinia clinical gamma camera.

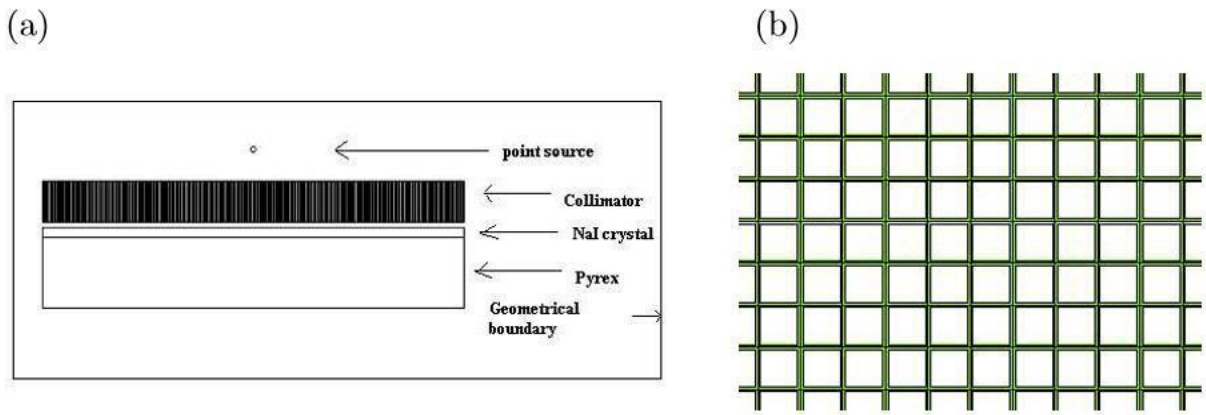

Figure 2: The MCNPX geometrical model of the gamma camera: (a) a side view, (b) a top view (not to scale) demonstrating the geometry of the LEHR parallel-hole collimator plotted from the MCNPX code.

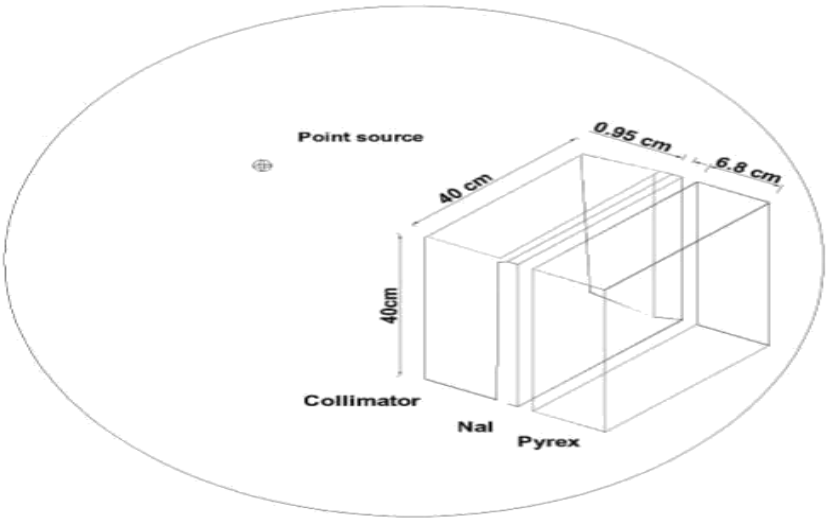

Figure 3: The MCNPX model of the LEHR parallel-hole collimator gamma camera including the geometrical boundary

Table2: The LEHR parallel-hole collimator specifications

Parameters	Descriptions
Collimator design	Parallel square holes
Material	Material Lead
Septa thickness (t)	0.02 cm
Hole size (d)	0.15 cm
Hole length (l)	4.00 cm
collimator to detector distance (e)	0.575 cm

3. Results and Discussions

3.1 Verification of the Simulation

To validate the simulation data, an accurate and detailed knowledge of the Infinia gamma camera response function is required to have a good faith that the geometry and the results from the simulation are correct. To simulate the response function of the gamma camera detector, first the resolution function of the camera needed to be modeled. Both the energy deposition and the spatial resolution function of the gamma camera were assumed to be closely approximated by a Gaussian response. This meant that the both Gaussian energy blurring and Gaussian spatial blurring were considered in the simulation.

Firstly, the limited spatial resolution encountered in real imaging situations, the recorded (X, Y) spatial information is blurred. The spatial blurring was achieved by sampling a Gaussian distribution with FWHM=0.37 cm, corresponding to the intrinsic resolution as determined by the camera's manufacturer. In the real gamma camera, this effect is due to incorrect image recording by the PMT. For the simulated data the true (X, Y) spatial information is blurred by a Gaussian with σ=FWHM/2.35=0.1574. Similarly, recording of the energy deposition process is also subject to Gaussian broadening by sampling a Gaussian with energy dependent FWHM. The FWHM energy dependence was determined experimentally, using derived spectra from the aforementioned Infinia gamma camera. Various mono-energetic gamma sources (^{201}Tl, ^{57}Co, ^{99m}Tc and ^{51}Cr) ranging from 72-320 keV peak energies were experimentally imaged in air with no scattering material. The FWHM values of these energy spectra were fitted to function [20] relating the energy deposited with the FWHM of the energy response [20, 21]:

$$FWHM = n_1 \times E^{1-n_2} \qquad (5)$$

Where n1, n2 are values representing the best fit to the experimental data and the simulated results from the MCNPX, and E is the energy deposited. The above functional model was used in the Mat lab code for blurring the energy deposited. Based on the energy spectra measurements, using the actual Infinia gamma camera, and using Eq.5 the best fit was found with n1=0.35 and n2=0.23 as demonstrated in Figure 4.

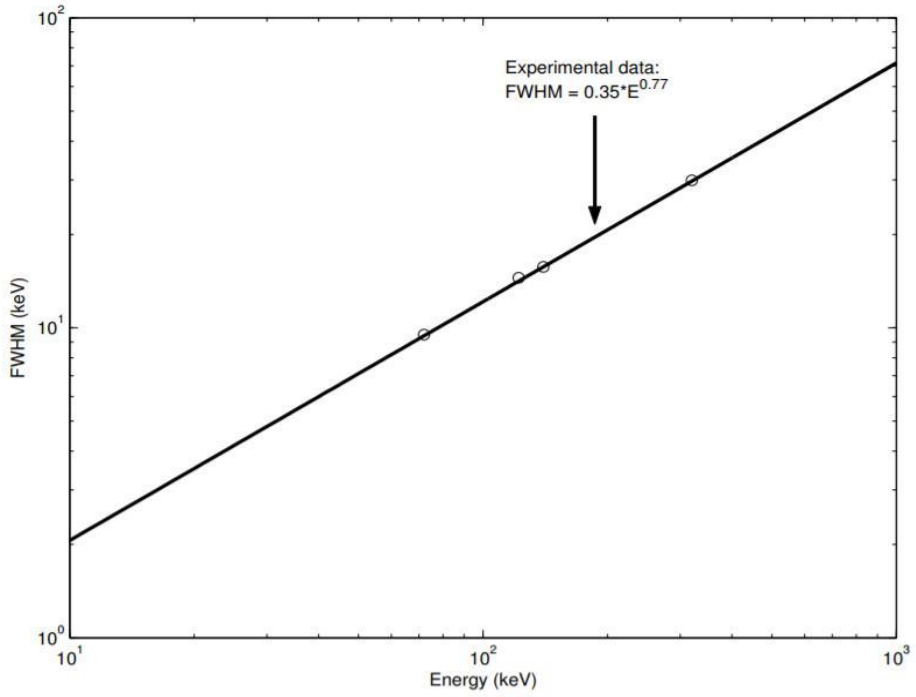

Figure 4: The relationship between the full energy peak FWHM and the energy deposited in the detector. Unfilled circles represent the experimental data

The γ-ray photons used in nuclear medicine usually suffer from Compton scattering as they travel through the scattering medium. As a result of this interaction process a photon loses energy. In addition, the NaI detector has an imperfect response to the incoming pulse. Thus, the energy deposition in the NaI crystal should be subjected to an acceptance window defined by 20% (± 10%) about the full energy peak. Because this symmetrical window is set around the full energy peak it is often called the photo peak window. For ^{99m}Tc, having gamma emission of 140 keV, the window is typically set between 126-154 keV. Photons which fall outside this window are rejected and do not contribute to the final image. In reality, the final projected image contains some proportion of scattered photon in the photo peak, due to statistical broadening.

Having constructed, tested the simulated geometry of the aforementioned Infinia γ camera, the initial step to be taken now is verify the simulation. This can be obtained by determining the simulated system Point Spread Function (PSF) and the energy spectra and comparing it with the experimental data. Using the PTRAC utility the simulated energy photo peak for a point source in air was first obtained and then compared with the corresponding experimental data obtain from the Infinia γ-camera. In both cases the incident radiation was mono-energetic (^{99m}Tc) at energy 140 keV. Figure 5 demonstrates the energy photo-peaks obtained from both the simulated data and the experimental data.

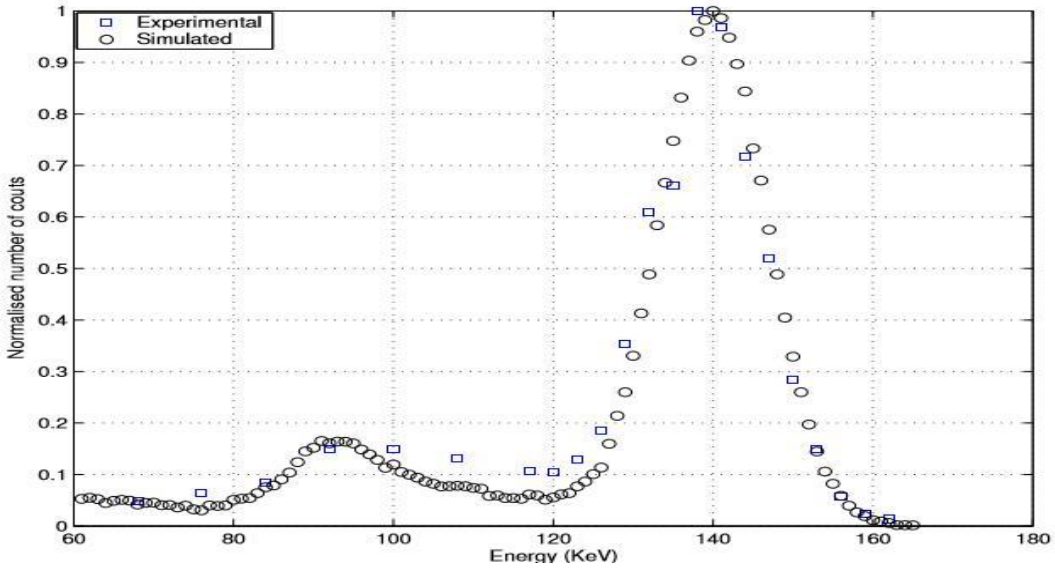

Figure 5: Comparison between the simulated and the experimental energy spectra for ^{99m}Tc of a small point source in air. The slight discrepancies between the two spectra are within the acceptable marginal error (i.e. 2-5 % of the FWHM)

Then the PSF is usually obtained from the 2D projected image of a point source in air. I can also be theoretically determined using the collimator equation and expressed as the FWHM. A set of MCS experiments of a point source in air located at various distances, (f), from the LEHR parallel-hole (of square-hole) were conducted. The chose distances were 2 cm, 5 cm, 10 cm, 25 cm, 50 cm and 75 cm and the number of histories simulated in each of these simulated work was 10^8. These were performed to investigate the spatial resolution as a function of distances from the γ-camera collimator. The same experiment

was a-priori performed using the aforementioned Infinia clinical imaging system that coupled to a hexagonal-hole LEHR collimator. Exemplar plots of the response from a point source in air at 25 cm distance obtained from both the MCS and the simulated data are shown in Fig. 6.

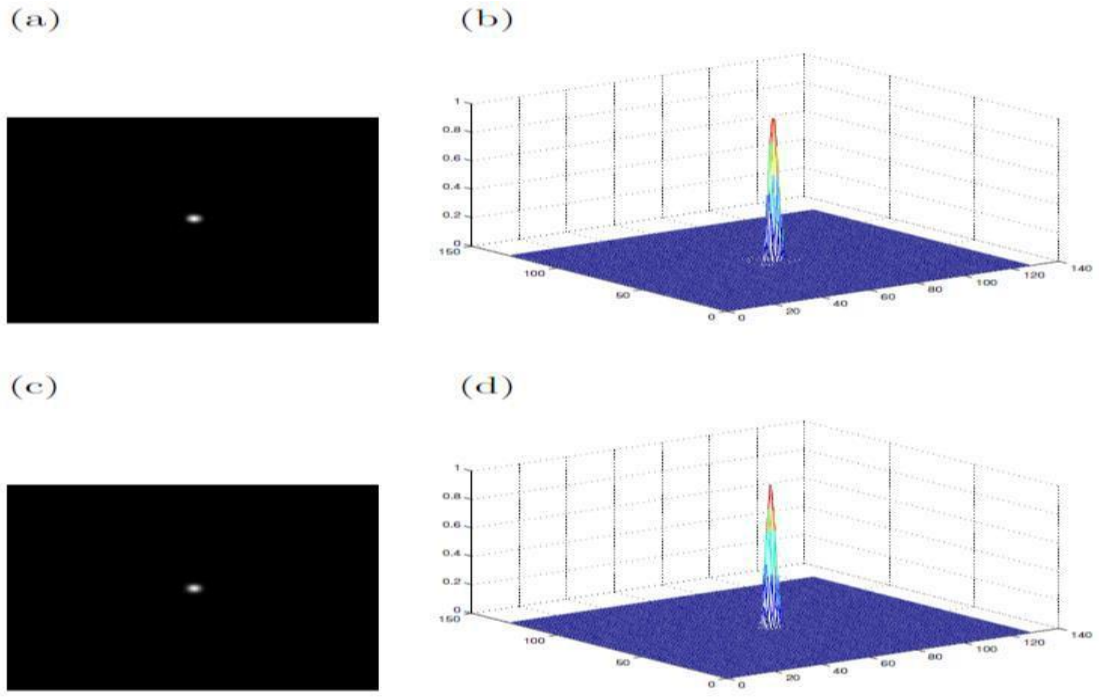

Figure 6: Exemplar plots of the response from a point source at 25 cm from the collimator face: (a) the image obtained experimentally using the Infinia gamma camera, (b) the corresponding 3D plot of the image, (c) The simulated image and finally (d) the corresponding 3D plot of the simulated image. These demonstrate that the simulated results agree with the experimental data.

Fig. 7 (a) and (b) shows the image profiles from both experiment and simulation of a point source in air separated by 10 and 50 cm from the collimator respectively. These demonstrate that simulation is in good agreement (i.e. ± 2 %) with the experimental data the spatial resolution expressed in FWHM were calculated from the simulated data and then compared with both the experimental data and the theoretical predictions. The theoretical resolution predictions were based on the collimator geometric spatial resolution equations proposed by Anger [22] and Webb [23] respectively. According to Anger the geometric resolution of the parallel hole collimator in terms of FWHM can be expressed as:

$$FWHM = \frac{d(l+f+e)}{l} \qquad (6)$$

Where is the hole diameter and is the source-to-collimator distance and is the distance between collimator and the center of the detector (commonly =0.575 cm), finally l is the collimator length or depth. Now if the parameters of Eq. 6 are replaced with the values shown in table 2 then the equation becomes FWHM = 0.038f +0.172. Similarly, Webb [23] suggested a similar equation but he ignored the e term as:

$$FWHM = \frac{d(l+f)}{l} = 0.038f + 0.0150 \qquad (7)$$

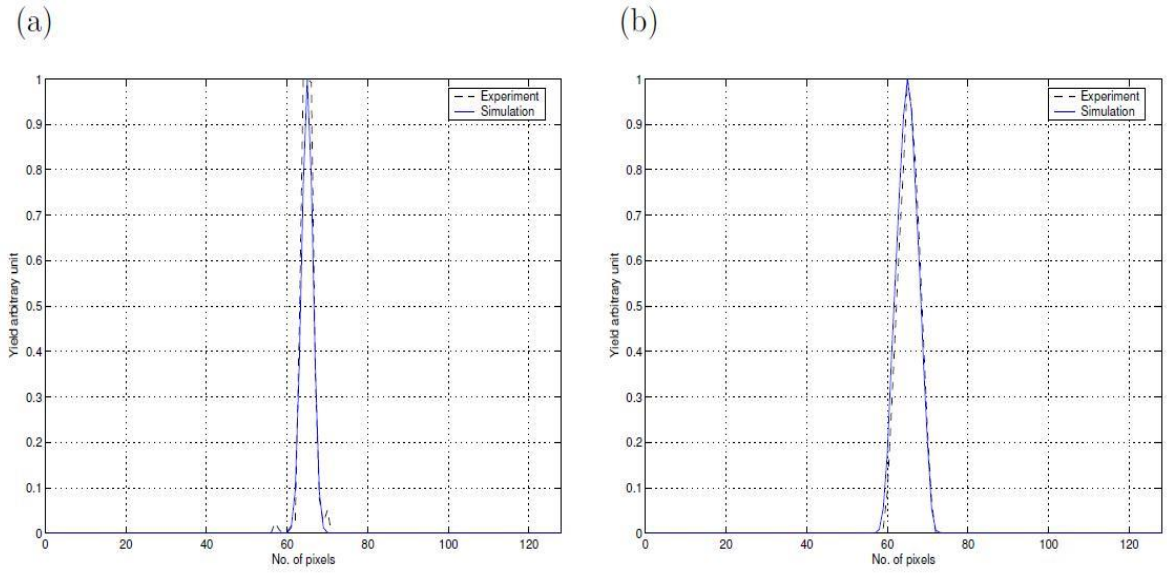

Figure 7: Exemplar profiles of the PSF from a point source obtained using MCS and real experiment using the Infinia gamma camera: (a) the point source located at 10 cm from the collimator, (b) the point source separated from the collimator by 50 cm. This demonstrates that the closer the points source from the collimator the sharper the PSF

The above theoretical equations (Eq. 6 & Eq. 7) defined by Webb and Anger suggest that the spatial resolution of the parallel-hole collimator can be improved by placing the source close to the collimator. Thus, both equations seem to have a linear relationship [23].

Using the least square error line fit to the experimental and simulated data gives this equation FWHM = 0.038f + 0.210 as plotted in Fig. 8. This also shows the variation of the spatial resolution in term of the FWHM for the LEHR parallel-hole collimator. The presented results are for the simulated and experimental data compared with the Anger and Webb theoretical equations. These demonstrated the fall off of the spatial resolution with increasing the distance of the source from the collimator. Fig. 8 demonstrates good agreement between the simulated and experimental data although the simulated collimator had a square hole compared with the hexagonal hole in the case of experimental data. This is also confirmed and agrees with that concluded by Devries [24] that on average both the square hole and the hexagonal hole approximately give the same result.

Figure 8 also show that the model used for the experimental and the simulated data also agree with Webb and Anger Model. The slight differences (less than 5%) between the model used here and the Webb and Anger models are expected. This is because both theoretical models given by Anger and Webb are geometrical models and neglects anything else. However, the model used for the experimental and simulated data are more realistic as it includes the degradation effect of the camera physics. This is because in both cases the imaging detector was based on NaI and this is responsible for worsening the spatial resolution.

This simulated camera model was used as a benchmark for the subsequent work with CA. The same camera model has been used after replacing the LEHR collimator with CA.

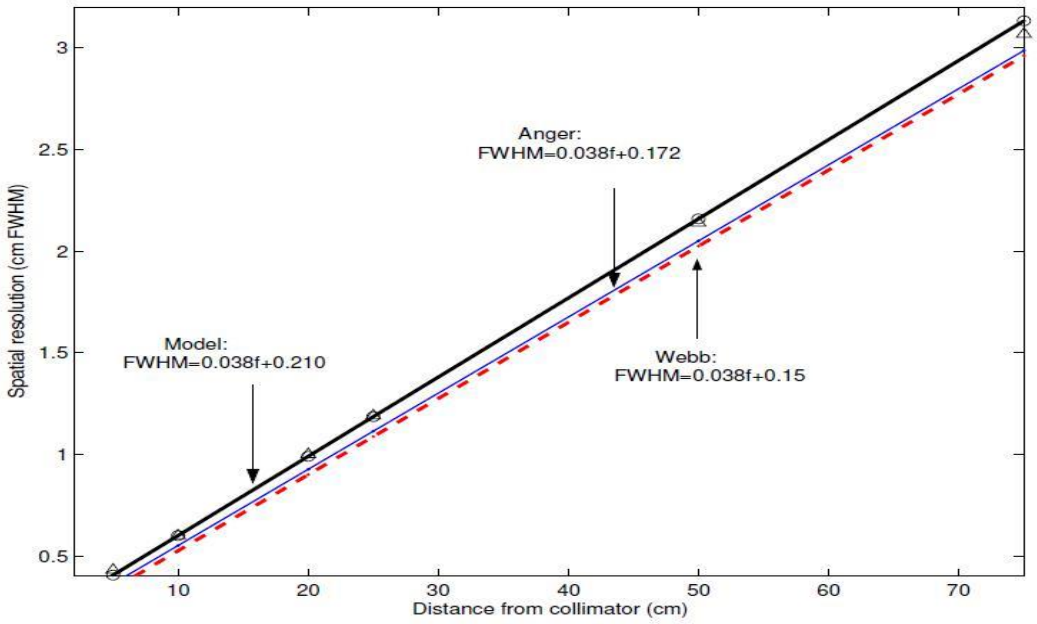

Figure 8: The spatial resolution in terms of the FWHM of an infinitesimally small point source of ^{99m}Tc in air versus imaging distance for experimental (unfilled triangle) and simulated results (unfilled circle) compared with theoretical models proposed by Anger and Webb.

4. Conclusion

The obtain results using MSC and real experiment using the Infinia gamma camera demonstrate accurate construction, testing and verification of the simulated geometry. It describes the design and the development of the MCS method used in this work. The first part describes the structure of the simulation code system. The second part presents the simulation method and code verification for modeling the imaging detector. The final part highlights the different geometries used in this initial work for modeling the exemplar Infinia gamma camera. Thus, closer agreement in term of PSF and energy spectra respectively was demonstrated. The slight discrepancy between the two is within the acceptable marginal error (i.e. 2-5 % of the FWHM).

References

1. Rudat V, Brune-Erbe I, Noureldin A, Bushnag Z, Almuraikhi N, Altuwaijri S. Epidemiology of breast cancer patients at a tertiary care center in the Eastern Province of Saudi Arabia, Gulf J Oncolog., 1(11):45-9, 2012.

2. Hamdan NA, Ravichandran K, Dyab AR., Breast cancer survival in Riyadh, Saudi Arabia, 1994-1996"., IARC Sci Publ;(162):179-81, 2011.

3. Magrath I (2004). International network for cancer treatment and research (INCTR). Available online at: www.inctr.org, publications/ 2002_v03_n01_s02.shtml, 2003.

4. Kahan E, Ibrahim AS, El Najjar K, et al., Cancer patterns in the Middle East-special report from the Middle East Cancer Society. Acta Oncol, **36**, 631-6, 1997.

5. The American cancer society, Cancer facts and Figures 2006, [http://www.cancer.org], retrieved on September. 2006.

6. Cavalli F., Hansen H.H. and Kaye S.B., Textbook of Medical Oncology, Martin Dunits Ltd. ISBN: 1853172901, 1998.

7. Parkin DM, Bray F, Ferlay J and Pisani P.Global. Cancer Statistics, CA Cancer 2005; 55:74-108,2002.

8. Akhtar S S, Lolita Malig Reyes. Cancer in Al-Qassim, Saudi Arabia: A Retrospective Study (1987-1995,Ann Saudi Med 17(6):595-600, 1997.

9. Schillaci O., and Buscombe J.R., "Breast scintigraphy today: indications and limitations" European Journal of Nuclear Medicine and Molecular Imaging, 31, S35-S45,2004.

10. Wiesenberger A.G., Barbosa F., Green T.D., Hoefer R., Keppel C., Kross B., Majewski S., Popor V.,Wojcik R., and Wymer D.C., "A Combined Scintimammography/Stereotactic Core Biopsy X-ray", Nuclear Science Symposium Conferece Record, 3, 2000.

11. Fondrinier E., Muratet J.P., Anglade E., Fauvet R., Breger V., Lorimier G., and Jallet P., "Clinical experience with ^{99m}Tc-MIBI scintimammography in patients with breast microcalcifications", Breast, 13, 4,316-320, 2004.

12. Schillaci O., Scopinaro F., Spanu A., Donnetti M., Danieli R., Di Luzio E., Madeddu G., and David V.,"Detection of axillary lymph node metastases in breast cancer with ^{99m}Tc tetrofosm inscintigraphy",International Journal of Oncology, 20, 3,483-487, 2002.

13. Briesmeister J.F., Ed., MCNPC4B2 Monte Carlo N-Particle Transport Code System Report CCC-660, Los Alamos National Laborator, 1998.

14. Ljungberg M., Strand S.E., King M.A., (Eds), Monte Carlo Calculations in Nuclear Medicine: Applications in Diagnostic Imaging, Institute of Physics Publishing, Bristol, 1998.

15. Zaidi H., "Relevance of accurate Monte Carlo modeling in nuclear medical imaging", Medical Physics, 26, 574-608, 1999.

16. Briesmeister J.F., Ed., MCNP-A General Monte Carlo N-Particle Transport Code, Version 4B, LA-12625-M, 1997.

17. Knoll G., Radiation Detection and Measurement,3rd ed., John Wiley Inc., New York, USA, 1999.

18. Saripan M.I., Wells K., Petrou M., Alnafea M.A. and Guy M., "Design of a Multi hole collimator gamma camera model for use in Monte Carlo simulation", Proceeding of the Medical Image Understanding and Analysis, 1, 87-90, 2005.

19. DeVries D. J, & Moore S.C.," Development and validation of a Monte Carlo simulation of photon transport in an Anger camera", IEEE Transaction on Medical Imaging, 9, 430-438, 1990.

20. Westmore M. A, "Study into the Feasibility of Applying Symmetric Spectral Deconvolution Techniques to Gamma Camera Data", Master's thesis, Department of Physics, University of Surrey, September 2003.

21. Beattie R. J. D, & Byrne. J, "A Monte Carlo program for evaluating the response of a scintillation counter tomonoenergetic gamma rays" Nuclear Instruments and Methods 104, 163168, 1972.

22. Anger H. O., "Scintillation camera with multichannel collimators", Journal of Nuclear Medicine, 5, 515-531, 1964.

23. Webb S., the Physics of Medical Imaging, Institute of Physics Publishing, Bristol and Philadelphia. ISBN: 0-85274-349-1, 1988.

24. DeVries D. J., & Moore S.C., "Comparison of hexagonal hole and square hole collimator by Monte Carlo simulation", IEEE Nuclear Science Symposium Conference,3, 52-56, 2000.